# Motility of keratocyte cells: asymptotic and numerical analysis via a phase field model

Matthew Mizuhara

The Pennsylvania State University
**Adviser**: Leonid Berlyand
**Other collaborators**: Volodymyr Rybalko, Lei Zhang

May 7, 2015

# Outline

1. Biological motivation
   - complex mechanisms $\Rightarrow$ competition of forces
2. Phase-field model
   - coupled equations for cell motility
3. Sharp interface limit
   - curvature motion $\Rightarrow$ development of non-linear contribution
4. Analytical/numerical results

# Motile cells

**Keratocyte cells:**[1] found in human cornea, fish scales. Central focus of modern experiments; move by *crawling* on substrate

**Importance** - integral to various biological responses
e.g., **healing corneal wounds**

**Ideal cells for experiments/modeling:**

1. Travel in straight lines
2. Self-propagate many times their own cell lengths
3. Maintain stereotypical shape during motion

[1] Typical length scale: $100 \mu m$

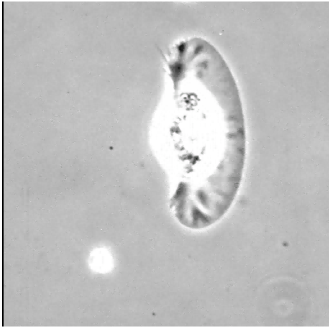

Movie of steady keratocyte motion
Source: EL Barnhart

# Overall cell structure

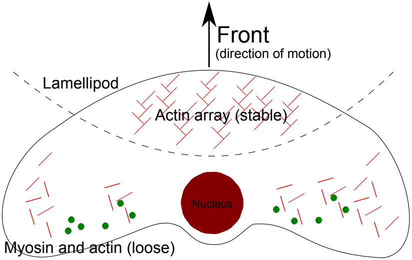


- Actin (protein) filaments protrude front of the cell
- Surface tension contributes to cell shape ⇒ tension minimized when cell is circular
- Ion transport enforces volume preservation (osmotic regulation)
- **Remark:** Mathematical model should shed light on these complex biological/physical interactions

# Phase-field model

Aronson, et al. (2011) used a *phase-field approach* to model cell motility

**Model:** *Phase-field variable*, $\rho(x,t)$ - describes location of the cell; takes value 1 inside the cell and 0 outside with a smooth $\varepsilon$-width transition at the boundary

*Vector field*, $P(x,t)$ - polar orientation of the actin filaments

This model is accurate and simpler than previous models (no matching BC at interface)

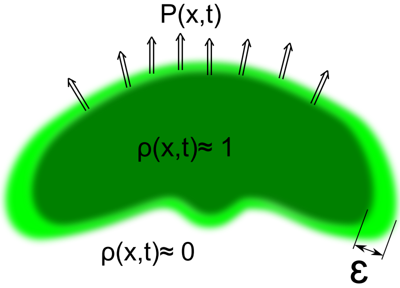

# Phase-field model

$\Omega \subset \mathbb{R}^2$ - bounded smooth domain (large substrate)

$$\begin{cases} \dfrac{\partial \rho_\varepsilon}{\partial t} = \Delta \rho_\varepsilon - \frac{1}{\varepsilon^2} W'(\rho_\varepsilon) - P_\varepsilon \cdot \nabla \rho_\varepsilon + \lambda_\varepsilon(t) \\ \dfrac{\partial P_\varepsilon}{\partial t} = \varepsilon \Delta P_\varepsilon - \frac{1}{\varepsilon} P_\varepsilon - \beta \nabla \rho_\varepsilon \end{cases} \text{in } \Omega \qquad (1)$$

Boundary conditions: $\partial_\nu \rho_\varepsilon = 0$ and $P_\varepsilon = 0$
$W(\rho) = \frac{1}{4}\rho^2(1-\rho)^2$ - double equal well potential ($\rho = 1, 0$),
$\beta$ - contains all physics (actin protrusion strength and polymerization rate, adhesion),
$\varepsilon$ - width of the transition layer,

$\lambda_\varepsilon(t) := \frac{1}{|\Omega|} \int_\Omega \left( \frac{1}{\varepsilon^2} W'(\rho_\varepsilon) + P_\varepsilon \cdot \nabla \rho_\varepsilon \right)$ - volume constraint

**Distinct features:** gradient coupling, non-local mass preservation

Take limit $\varepsilon \to 0$ in (1) $\Rightarrow$ sharp interface limit equation

# Features of current equations

In recent work of Berlyand, et al. (2014) sharp interface limit of (1) derived:

$$V = \kappa + \frac{\beta}{c_0}\Phi(V) - \frac{1}{|\Gamma(t)|}\int_{\Gamma(t)} \left(\kappa + \frac{\beta}{c_0}\Phi(V)\right) ds. \qquad (2)$$

$V$ - inward normal velocity, $\kappa$ - curvature, $\beta$ - physical parameter, $c_0 = \sqrt{3/2}$ (depends only on double-well potential $W$)
$\Phi$ - known non-linear function
*Equation* (2) *is an equation for the evolution of a planar curve* $\Gamma$ *(i.e., given* $\Gamma$*, one computes* $\kappa$ *and* $V$*)*

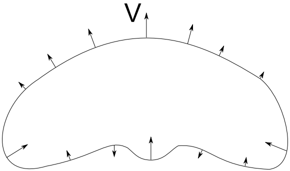


**Two regimes:** Subcritical $\beta < \beta_{cr}$, supercritical $\beta > \beta_{cr}$

# Comparison of subcritical/supercritical $\beta$

Consider $F(V) := V - \frac{\beta}{c_0}\Phi(V)$

**Subcritical regime** $(\beta < \beta_{cr})$**:** $F$ is monotone
**Supercritical regime** $(\beta > \beta_{cr})$**:** $F$ is non-monotone

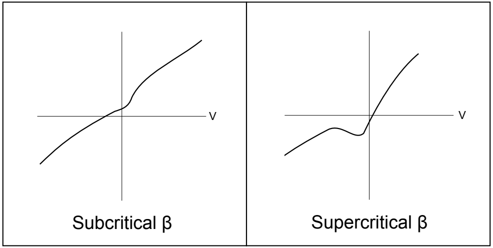


- Supercritical $\beta \Rightarrow$ Non-uniqueness of solutions, hysteresis

# Goals (MM, Berlyand, Rybalko, Zhang)

For $\beta < \beta_{cr}$, investigate existence, uniqueness and regularity of evolution of curves $\Gamma(t)$ for equation

$$V = \kappa + \frac{\beta}{c_0}\Phi(V) - \frac{1}{|\Gamma(t)|}\int_{\Gamma(t)}\left(\kappa + \frac{\beta}{c_0}\Phi(V)\right) \qquad (3)$$

**Analytical objectives:**

- Prove existence of curves traveling via (3)
- Study traveling wave solutions of (3)

**Numerical objectives:**

- Develop algorithm to compute evolution of curves
- Quantify effect of physical parameter $\beta$ on net motion
- Study how initial geometry affects net motion

# Analytical results

## Theorem 1

Let $0 < \beta < \beta_{cr}$. Given $\Gamma_0 \in W^{1,\infty}$, there exists $T = T(\Gamma_0) > 0$ such that a family of curves $\Gamma(t) \in H^2$ exists for $t \in (0, T]$ satisfying the evolution equation (3) with $\Gamma(0) = \Gamma_0$.

*Proof idea:* Write the evolution equation as a PDE and prove existence for smooth ($H^2$) data. Passing to $W^{1,\infty}$ requires uniform estimates (independent of $H^2$ initial data) based on a maximum principle argument and classical results on Hölder continuity of solutions to quasilinear PDEs.

**Remark:** $W^{1,\infty}$ initial conditions $\Rightarrow$ corners

## Theorem 2

Let $0 < \beta < \beta_{cr}$. There are no traveling wave solutions of (3) other than trivial stationary circles.

**No moving traveling waves** $\Rightarrow$ can we still observe *transient motion* of curves for subcritical $\beta$?

# Numerical Results

**Main difficulty:** Discretizing curve gives rise to coupled system of non-linear equations $\Rightarrow$ hard to solve and preserve volume

**Resolution:** Develop *splitting scheme* which alternatively resolves 1) non-linearity 2) volume preservation

**Experiment:** Fix $\Gamma(0)$. Compute $\Gamma(t)$ propagating via (3) for $0 < \beta < \beta_{cr}$; compare to $\beta = 0$ (volume preserving curvature motion)

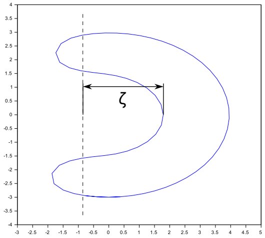


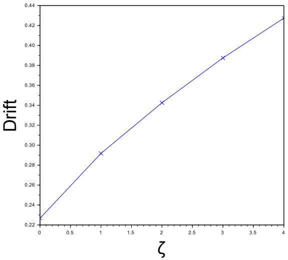


**Observations:** Curves propagating via (3) with $0 < \beta < \beta_{cr}$
(i) converge to a steady-state circle
(ii) transient motion; distance proportional to 1) $\beta$ and 2) asymmetry $\zeta$

# Conclusions

- Aronson, et al. proposed a *phase-field model* to describe keratocyte cell motility
- Berlyand, et al. derived the *sharp interface limit equation* $\Rightarrow$ non-linear, non-local equation describing evolution of planar curves
- We investigate this sharp interface limit equation in the subcritical $\beta < \beta_{cr}$ regime:
  - **Analytical results:** existence of solutions, non-existence of traveling waves
  - **Numerical results:** convergence to steady-state circle, drift distance depending on physical parameter $\beta$ and initial geometry

# Thank you

**Thank you for your attention!**

This work is partially supported by the Department of Defense (DoD) through the National Defense Science & Engineering Graduate Fellowship (NDSEG) Program

# Appendix

# Splitting scheme

Given a curve $\Gamma$, discretize it by $N$ points: $p_i = (x_i, y_i)$, $i = 1, \ldots, N$.
Naive discrete approximation:

$$V_i = \kappa_i + \beta\Phi(V_i) - \frac{1}{|\Gamma|}\sum_{j=1}^{N}\kappa_j + \beta\Phi(V_j)dS, \tag{4}$$

$\kappa_i, |\Gamma|, dS$ - discrete curvature, curve length, and line element, resp.
**Non-linearity** and **area preservation** $\Rightarrow$ level-set methods not available
Introduce the following *splitting scheme:*

1. Fix an auxiliary parameter $C \in \mathbb{R}$
2. Use an iteration method to solve

$$\tilde{V}_i = \kappa_i + \beta\Phi(\tilde{V}_i) - C \quad \textit{(local equation)} \tag{5}$$

3. Temporarily update $\Gamma$ by the velocity profile $\tilde{V}$: $\tilde{p}_i = p_i + \tilde{V}_i\mathbf{n}_i$, $\mathbf{n}_i$ - discrete inward pointing normal. Compute change in area
4. Adjust auxiliary parameter $C$; repeat (2)-(3) until area is preserved

# Parametrization of curve

Let $\tilde{\Gamma}_0$ be a $C^4$ smooth reference curve in a small neighborhood of $\Gamma_0$ with curvature $\kappa_0$ and let $\tilde{\Gamma}_0$ be parametrized by arc length parameter $\sigma \in I$. Then

$$\Gamma(\sigma, t) = \tilde{\Gamma}_0(\sigma) + u(\sigma, t)\nu(\sigma),$$

with $\nu$ the normal vector to $\tilde{\Gamma}_0$ and $u$ solves

$$u_t - \frac{S}{1 - u\kappa_0}\Phi\left(\frac{1 - u\kappa_0}{S}u_t\right) = \frac{S}{1 - u\kappa_0}\kappa(u) - \frac{S}{(1 - u\kappa_0)L(u)}\left(\int_I \Phi\left(\frac{1 - u\kappa_0}{S}u_t\right) S d\sigma + 2\pi\right),$$

where $S = \sqrt{u_\sigma^2 + (1 - u\kappa_0)^2}$, and $L(u)$ is the total arc length of $u$.

# Result on asymptotic equation

Consider the 1d model:

$$\begin{cases} \dfrac{\partial \rho_\varepsilon}{\partial t} & = \partial_x^2 \rho_\varepsilon - \dfrac{W'(\rho_\varepsilon)}{\varepsilon^2} + P_\varepsilon \partial_x \rho_\varepsilon + \dfrac{F(t)}{\varepsilon}, \quad x \in \mathbb{R}^1 \\ \dfrac{\partial P_\varepsilon}{\partial t} & = \varepsilon \partial_x^2 P_\varepsilon - \dfrac{1}{\varepsilon} P_\varepsilon + \beta \partial_x \rho_\varepsilon. \end{cases} \tag{6}$$

**Note:** Problem now exists on $\mathbb{R}$ and $F(t)$ is an arbitrary function.

Let $\theta_0$ be the standing wave solution $\theta_0'' = W'(\theta_0)$.

**Theorem.** *Let $\rho_\varepsilon$ and $P_\varepsilon$ solve (6) on $[0, T]$ with "nice" initial data. For $\beta$ sufficiently small, we have $\rho_\varepsilon = \theta_0\left(\frac{x - x_\varepsilon(t)}{\varepsilon}\right) + \varepsilon \rho_\varepsilon^{(1)}$ where $x_\varepsilon(t)$ is the interface location between 0 and 1 phase. Moreover $x_\varepsilon(t) \to x_0(t)$ with*

$$-c_0 \dot{x}_0(t) = \beta \Phi(\dot{x}_0(t)) + F(t), \Phi(-V) := \frac{1}{\beta} \int \psi |\theta_0'|^2 dy$$

# Proof outline

Approximate $\rho_\varepsilon$ and $P_\varepsilon$ as

$$\rho_\varepsilon \approx \theta_0\left(\frac{x - x_\varepsilon(t)}{\varepsilon}\right) + \sum_{i=1}^{N} \varepsilon^i \theta_i\left(\frac{x - x_\varepsilon(t)}{\varepsilon}, t\right), \quad P_\varepsilon \approx \sum_{i=0}^{N} \varepsilon^i \psi_i\left(\frac{x - x_\varepsilon(t)}{\varepsilon}, t\right).$$

Expand $x_\varepsilon(t)$ in an $\varepsilon$-series; substitute and match powers of $\varepsilon$:

$$\begin{aligned}
\theta_0'' &= W'(\theta_0) \\
-\theta_1'' + W''(\theta_0)\theta_1 &= -V_0\theta_0' + \Psi_0\theta_0' + F(t) \\
-\theta_2'' + W''(\theta_0)\theta_2 &= -V_1\theta_0' - V_0\theta_1' - \frac{W'''(\theta_0)}{2}\theta_1^2 + \Psi_0\theta_1' + \Psi_1\theta_0'
\end{aligned}$$

and

$$\begin{aligned}
\Psi_0'' - V_0\Psi_0' - \Psi_0 &= -\beta\theta_0', \\
\Psi_1'' - V_0\Psi_1' - \Psi_1 &= -\beta\theta_1' + V_1\Psi_0' + \dot{\Psi}_0, \\
\Psi_2'' - V_0\Psi_2' - \Psi_2 &= -\beta\theta_2' + V_1\Psi_1' + V_2\Psi_0' + \dot{\Psi}_1.
\end{aligned}$$

# Eigenvalue of linearized Allen-Cahn

Since $\theta_0'' = W'(\theta_0)$ then $\theta_0'$ is a zero eigenfunction of the operator

$$\mathcal{L}(f) = f'' - W''(\theta_0)f.$$

The Fredholm alternative implies that $g \in \operatorname{Im}\mathcal{L}$, if and only if $g \in (\operatorname{Ker}\mathcal{L})^\perp$. One can show $(\operatorname{Ker}\mathcal{L})^\perp = \operatorname{span}\{\theta_0'\}$. In other words, the equations for $\theta_i$ have solutions if and only if

$$\int(-V_0\theta_0' + \Psi_0\theta_0' + F(t))\theta_0' = 0,$$

$$\int(-V_1\theta_0' - V_0\theta_1' - \frac{W'''(\theta_0)}{2}\theta_1^2 + \Psi_0\theta_1' + \Psi_1\theta_0')\theta_0' = 0.$$

This gives the correct interface equation. The result follows by completing estimates on energy.

# Classical result

Gage proved that a convex curve moving under area preserving curvature motion will converge to a circle exponentially.
Let $L = L(t)$ be the length of the curve at time $t$, $A$ - area, $k$ - curvature, $N$ - normal vector

1. $L_t = -\int \langle V, kN \rangle ds$
2. $L_t \leq 0$ for all $t$ (the curve is length shortening)
3. $\left(\frac{L^2}{A} - 4\pi\right) \leq Ce^{\frac{-2\pi}{A}t}$

Using the Bennesen inequality,

$$\left(\frac{L^2}{A} - 4\pi\right) \geq \frac{\pi^2}{A}(r_{out} - r_{in})^2$$

where $r_{out}$ is the radius of the encompassing circle and $r_{in}$ is the radius of the inscribed circle, the result follows.

It is important to note that he also must prove that convex curves remain convex and singularities do not develop.

# Small $\beta$

We expect for small values of $\beta$ that a similar result should hold. We are currently working to prove that (2) gives rise to length shortening flow.

If we apply similar methods as Gage, we compute the following

$$L_t = -\int k^2 + \frac{4\pi^2\nu^2}{L} + \beta \int \left(\frac{2\pi\nu}{L} - k\right) \Phi \leq -\theta + \beta\theta^{1/2}.$$

Here, $\theta = -\int k^2 + \frac{4\pi^2\nu^2}{L}$ is a measure of how “far” we are from a circle. If length is decreasing then $\theta \to 0$. This would imply that $\beta \to 0$. Thus, new techniques are required to complete this result.

# Cyclic view of motion

**Orientation** - choice of direction based on external cues (chemical gradients, mechanical deformations)

**Protrusion** - extension of cell membrane in direction of motion. Polymerization of actin filaments - backbone of protrusion

**Adhesion** - attachment of a cell to the extra-cellular matrix (ECM)

**Retraction** - contraction of actomyosin cytoskeleton

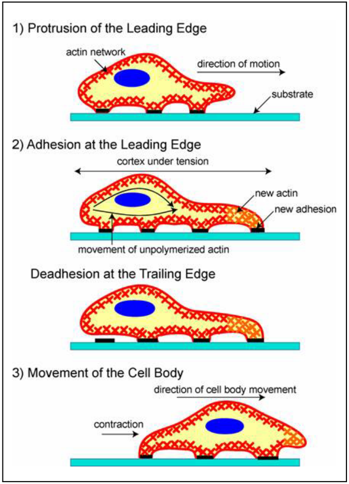

# Plan of Computational Approach

Consider

$$V = \kappa + \frac{\beta}{c_0}\Phi(V) - \frac{1}{|\Gamma(t)|}\int_{\Gamma(t)} \left(\kappa + \frac{\beta}{c_0}\Phi(V)\right).$$

Let $f(V) := \frac{1}{c_0}\left(\Phi(V) - \frac{1}{|\Gamma|}\int_{\Gamma(t)} \Phi(V)\right)$.
Perturbation theory motivates iterative scheme:

$$V_0 = \kappa - \frac{1}{|\Gamma(t)|}\int_{\Gamma(t)} \kappa,$$

$$V_1 = V_0 + \beta f(V_0),$$

$$\vdots$$

$$V_n = V_0 + \beta f(V_{n-1}).$$

# Convergence for Small $\beta$

Observe

$$\begin{aligned}
\|V_n - V_{n-1}\|_{L^1} &= \|\beta(f(V_{n-1}) - f(V_{n-2}))\| \\
&= \left\| \frac{\beta}{c_0} \left( \Phi(V_{n-1}) - \Phi(V_{n-2}) - \frac{1}{|\Gamma|} \int_{\Gamma(t)} \Phi(V_{n-1}) - \Phi(V_{n-2}) \right) \right\| \\
&\leq \frac{2\beta}{c_0} \left( \int |\Phi(V_{n-1}) - \Phi(V_{n-2})| \right) \\
&\leq \frac{2\beta}{c_0} |\Phi'(V)|_{L^\infty} \|V_{n-1} - V_{n-2}\|_{L^1}
\end{aligned}$$

So for $\beta$ small enough this iterative scheme converges.

# Lamellipodia

The *lamellipod* is the leading edge of the cell which drives locomotion.

The *dendritic-nucleation hypothesis* predicts a precise pattern of *angular branching* of *actin filaments*.

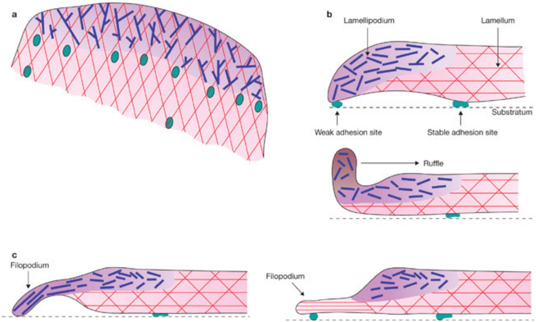


The major conclusion from this model is that cell motion is dictated by an array of progressing filaments, not by individual filaments.

# Contraction

Another key protein in cell motility is *myosin*, responsible for contraction.

Essentially, it uses energy from the ATP hydrolysis to enact a force on existing actin filaments.

# Contraction

Another key protein in cell motility is *myosin*, responsible for contraction.

Essentially, it uses energy from the ATP hydrolysis to enact a force on existing actin filaments.

Actin disassembly leads to piling of "unorganized" actin filaments at the rear of the cell on which myosin can act, effectively pulling the rear of the cell forward.

# Residuals

Modify the expressions

$$\rho_\varepsilon = \tilde{\rho}_\varepsilon + \varepsilon^\alpha u_\varepsilon, \text{ and } P_\varepsilon = \tilde{P}_\varepsilon + \varepsilon^\alpha Q_\varepsilon.$$

Plugging in these expressions into the original equation, we get

$$\frac{\partial u_\varepsilon}{\partial t} = \frac{u_\varepsilon''}{\varepsilon^2} - \frac{V_0 u_\varepsilon'}{\varepsilon} - \frac{W''(\theta_0)u_\varepsilon}{\varepsilon^2} - \frac{W'''(\theta_0)u_\varepsilon \theta_1}{\varepsilon} + \frac{\Psi_0 u_\varepsilon'}{\varepsilon} + \frac{Q_\varepsilon \theta_0'}{\varepsilon} + R_\varepsilon(t,y). \tag{7}$$

and

$$\frac{\partial Q_\varepsilon}{\partial t} = \frac{Q_\varepsilon''}{\varepsilon} - \frac{V_0 Q_\varepsilon'}{\varepsilon} - \frac{Q_\varepsilon}{\varepsilon} + \frac{\beta u_\varepsilon'}{\varepsilon} + \varepsilon^{N-\alpha} m_\varepsilon(t,y). \tag{8}$$

Our goal is to obtain bounds on $u_\varepsilon$ and $Q_\varepsilon$.

# Proof Outline

**Proof idea**:1. Write $u_\varepsilon(y,t) = \theta_0'(y)[\nu_\varepsilon(t,y) + \xi_\varepsilon(t)]$ where $\theta_0'\nu_\varepsilon$ is orthogonal to $\theta_0'$.
This *factoring* of $u_\varepsilon$ is useful because it allows us to use a modified **Poincaré inequality**.
2. Then, can obtain a bound

$$\frac{d}{2dt}\|u_\varepsilon\|_{L^2}^2 + \frac{1}{2\varepsilon^2}\int (\theta_0')^2(\nu_\varepsilon')^2 dy \leq C\xi_\varepsilon^2 + \frac{1}{\varepsilon}\left[\int Q_\varepsilon(\theta_0')^2(\nu_\varepsilon + \xi_\varepsilon)dy - \int \psi_0'(\theta_0')^2 dy \xi_\varepsilon^2\right] + \int R_\varepsilon \theta_0'(\nu_\varepsilon + \xi_\varepsilon)dy.$$

3. To estimate $u_\varepsilon$, only must bound $\frac{1}{\varepsilon}$ terms. (Use that $\psi_0$ solves $\psi_0'' - V_0\psi_0' - \psi_0 = -\beta\theta_0'$.)
4. Bound the remaining terms to get the energy estimates:

# Proof End

Define energies

$$\mathcal{E}_\varepsilon(t) = \int (\theta_0')^2 \nu_\varepsilon^2 dy + c_0 \xi_\varepsilon^2 + \frac{1}{c_p \beta^2 \varepsilon} \int B_\varepsilon^2 dy + \frac{1}{\varepsilon} \int D_\varepsilon^2 dy$$

$$\mathcal{D}_\varepsilon(t) = \frac{1}{8\varepsilon^2} \left\{ \int (\theta_0')^2 (\nu_\varepsilon')^2 dy + \int B_\varepsilon^2 dy + \int (B_\varepsilon')^2 dy + \int D_\varepsilon^2 dy + \int (D_\varepsilon')^2 dy \right\} + \left( \frac{\beta}{8} - c\beta^2 \right) \dot{\xi}_\varepsilon^2.$$

Then can show

$$\dot{\mathcal{E}}_\varepsilon + \frac{1}{2}\mathcal{D}_\varepsilon \leq c\mathcal{E}_\varepsilon + c\varepsilon\mathcal{E}_\varepsilon^{3/2} + c\varepsilon\mathcal{E}_\varepsilon^2 + c\varepsilon^6\mathcal{E}_\varepsilon^3 + c(\varepsilon + \varepsilon^2\mathcal{E}_\varepsilon^{1/2} + \varepsilon^4\mathcal{E}_\varepsilon^{3/2})\mathcal{D}_\varepsilon.$$

If $\mathcal{E}_\varepsilon(t) \leq c$ for $t \in [0, t*)$ then $\dot{\mathcal{E}}_\varepsilon \leq c\mathcal{E}_\varepsilon$. For small $\varepsilon$ the result holds.

# Actin protein

The cells on which we focus use *actin treadmilling* as a means of transportation (e.g. fish keratocytes).
*Actin* is a globular (spherical) protein which exists in two forms: G-actin and F-actin.


Actin Filament

*G-actin* is a monomer of actin ($\sim 5.4$ nm) containing a polarity: one end is barbed and the other is pointed (analogy is an ice-cream cone).

*F-actin* is a filament of actin formed by assembly of G-actin. The barbed end assembles and disassembles monomers two orders of magnitude faster than the pointed end (due to ATP binding).

# ATP capping and polarity

In the absence of *nucleotide hydrolysis*, the barbed and pointed ends of F-actin polymerize and depolymerize at the same rates.

However, G-actin binds to ATP at the barbed end and the following hydrolyzation occurs:

$$ATP \to ADP + P_i + \Delta E.$$

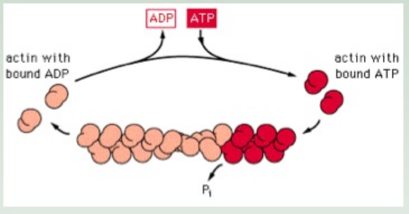

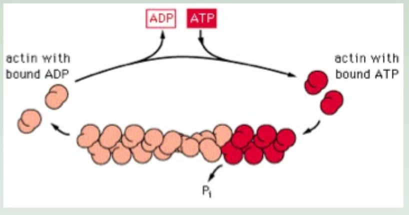


ADP-actin has the tendency to dissemble at the pointed end resulting in a net treadmill effect.

ADP-ATP re-charge occurs in the plasma membrane resulting in a basic mechanism for cell motility.

This cycle turns **chemical energy** into **mechanical energy**.